EPJ Web of Conferences **117**, 07023 (2016) DOI: 10.1051/epjconf/201611707023
NN2015

Charge-changing cross section measurement of neutron-rich carbon isotopes at 50 AMeV

D. T. Tran[1,2], T. T. Nguyen[2,3], I. Tanihata[1,4], H. J. Ong[1], M. Fukuda[5], N. Aoi[1], Y. Ayyad[1], H. Sakaguchi[1], J. Tanaka[1], P.Y. Chan[1], T. H. Hoang[1,2], T. Hashimoto[6], E. Ideguchi[1], A. Inoue[1], T. Kawabata[7], L. H. Khiem[2], K. Matsuta[5], M. Mihara[5], S. Momota[8], D. Nagae[9], A. Ozawa[9], P.P. Ren[10], S. Terashima[4], R. Wada[10], W.P. Lin[10] and T. Yamamoto[1]

[1] Research Center for Nuclear Physics, Osaka University, Japan
[2] Institute Of Physics, Vietnam Academy of Science and Technology, Hanoi, Vietnam
[3] Faculty of Physics and Engineering Physics, VNU-HCMUS, Vietnam
[4] Beihang University, Beijing, China
[5] Department of Physics, Osaka University, Osaka, Japan
[6] Institute for Basic Science, Daejon, Korea
[7] Department of Physics, Kyoto University, Kyoto, Japan
[8] Kochi University of Technology, Kochi, Japan
[9] Institute Of Physics, University of Tsukuba, Tsukuba, Japan
[10] Institute of Modern Physics, Lanzhou, China

Abstract

Charge Changing Cross Sections (CCCS or σ_{CC}) of neutron-rich carbon isotopes on carbon target were measured at low energy (50A MeV) for the first time. The consistency between Glauber calculation and experimental σ_{CC} of ^{12}C isotope at low energy region shows that proton distribution radii can be derived from CCCS at low energy.

© The Authors, published by EDP Sciences - SIF. This is an open access article distributed under the terms of the Creative Commons Attribution License 4.0 (http://creativecommons.org/licenses/by/4.0/).

1 Introduction

The world of atomic nuclei is governed by nuclear physics which can be described by nuclear structure models. The proton and neutron distribution radii of nuclei are good observables for testing nuclear structure models. The rms radii of proton distribution for some of the light and stable nuclei have been determined by isotope shift measurements [1–4]. However, applications of this method to unstable nuclei from B to Ne isotopes are extremely challenging due to the uncertainty in atomic physics calculation. The recent progress in Glauber model analysis enables the extraction of the matter distribution radii from interaction/reaction cross section (σ_{R}) [5]. The Glauber model can be extended to extract proton distribution radii from Charge-Changing Cross Sections (CCCS or σ_{CC}) on a known target. Eq.(1) shows the formula to calculate σ_{CC} in the Glauber model framework.

$$\sigma_{\mathrm{CC}} = \int d\mathbf{b}\,[1 - T(\mathbf{b})] \tag{1}$$

where $T(\mathbf{b})$ is transmission function:

$$T(\mathbf{b}) = \exp\left\{-\int d\mathbf{r}\rho_{\mathrm{Pp}}\left(\mathbf{r}-\mathbf{b}\right)\left[\sigma_{\mathrm{pp}}\rho_{\mathrm{Tp}}\left(\mathbf{r}\right)+\sigma_{\mathrm{pn}}\rho_{\mathrm{Tn}}\left(\mathbf{r}\right)\right]\right\}.$$

The formula includes five physical quantities: the projectile proton density $\rho_{\mathrm{Pp}}(r)$, the target one $\rho_{\mathrm{Tp}}(r)$, the target neutron density $\rho_{\mathrm{Tn}}(r)$, and the precisely determined bare proton-proton (σ_{pp}) and proton-neutron (σ_{pn}) total cross sections.

This extension has been shown to work well for stable nuclei and Li isotopes at high energy [6] and has been applied to Be [7], B [8] and C [9] isotopes at high energy region ($E > 200A$ MeV). Experimental results on proton distribution radii showed that increasing number of neutron in nuclei leads to increases in the proton distribution radii in He [1,3], Li [2], Be [4] and B [8] isotopes, especially in neutron-halo nuclei. The experimental results are consistent with the predictions of Antisymmetrized Molecular Dynamics (AMD) model [10]. However, the AMD calculation predicted that proton densities (radii) of C isotopes are almost constant. The weak N dependence of the proton radius indicates the insensitivity of the proton distribution to that of the neutrons.

However, the agreement between the zero-range Glauber calculation with the experimental values of reaction-cross section is not so good at intermediate energies even for stable nuclei, especially, the discrepancy at a few ten MeV/nucleon reaches almost 20%. To reduce such discrepancy, therefore, we used the finite-range optical limit approximation Glauber type calculation.

2 Experiment

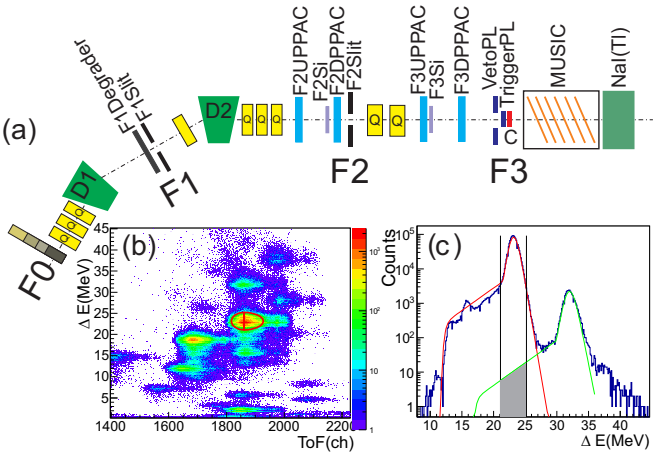

Figure 1: (a) Schematic view of the experiment setup. Identification spectrum of (b) ^{12}C before reaction target and (c) contamination estimation.

The experiment was performed at the EN course [11], RCNP, Osaka University using transmission method. In this method, the σ_{CC} is calculated as $\sigma_{\mathrm{CC}} = \frac{1}{t} \ln \left[\frac{1}{\gamma}\right]$, in which t is target thickness, γ is the ratio of the number of outgoing nuclei, which have the same atomic number with incoming nuclei (N_{sameZ}) to the number of incoming beam (N_{inc}). The detector setup is shown in fig. 1(a). Carbon-isotope beams were produced in separate runs by fragmentation of the ^{22}Ne primary beam at 80A MeV interacting with thick Be target ($1-5$ mm for different isotopes) located at F0. The interested isotope was selected in flight by setting the appropriate magnetic rigidity (Bρ) using dipole magnets D1 and D2. The beam energy was tuned by using combination of Be target, F1Degrader, F1Slit and determined using the Bρ values. The selected secondary beam was focused at F2 focal plane; contaminants were eliminated using a set of collimators at F2. The incoming beam (N_{inc}) was identified and counted by using the information of energy loss in a 320μm-thick silicon detector (F3Si) and time of flight (TOF) between the production target and a 100μm-thick plastic scintillator, which was also used as the trigger for data taking. The secondary beams were focused on a 450 mg/cm^2 carbon target placed at F3. The track and the spot of beam was provided by four Parallel Plate Avalanche Counters (PPAC) [12] located at F2 and F3. The particles that scattered at large angles after the last PPAC was rejected using a plastic veto and trigger counter, which have the same size and were located in front of the carbon target. The outgoing particles went through a MUlti Sampling Ionization Chamber (MUSIC) [13] before being stopped in a 7 cm-thick NaI(Tl) scintillator. The ΔE$-$E method was

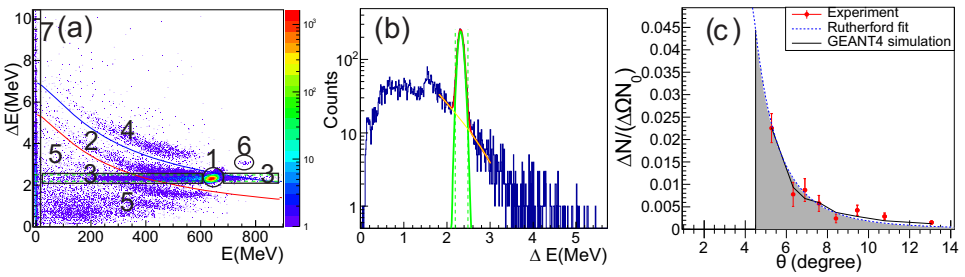

Figure 2: (color online). (a) Scattered particles identification, (b) background estimation of region 5 in region 3, (c) acceptance factor calculation.

used to identify and count the scattered particles (N_{sameZ}).

3 Results and discussion

The incoming particle was identified and counted by ΔE−TOF method (fig. 1(b)) with less than 0.1% of admixing of other nuclides due mainly to channelling effect in silicon crystal. We use MUSIC instead of Si detectors after the reaction target to avoid complication due to the channeling effect in silicon. The contaminants was estimated using the distribution obtained by selecting the contaminant events detected by the detector after the target. The contaminants contribute to cross section ranging from 0.1 to 3.5 mb depending on isotopes.

Particle identification of scattered particles is more complicated at low-energy region than at high energy. The outgoing particles were identified and categorized into 7 regions (fig. 2(a)): (1) beam-like particles, (2) elastic and inelastically scattered beam-like particles, (3) particles reacted in NaI(Tl), (4) proton-removed particles, (5) proton-picked-up particles, (6) contaminants, and (7) out-of-acceptance particles, which we did not detect. The number of events with the same Z as the incoming beam was calculated by summing the events in region 1, 2 and 3. To estimate the number of counts of light particles in region 3, the a Gaussian plus exponential background function was used to fit the experimental data (fig. 2(b)). The systematic uncertainties attributed to the background was bellow 1mb in final σ_{CC}.

The main systematic uncertainty, about 20% of the final σ_{CC}, is attributed to the uncertainty in the estimation of the "*unreacted*" particles (about 2%) that failed to reach the NaI(Tl) detector. To consider this effect, we introduced the acceptance factor (P) and the final σ_{CC} was deduced

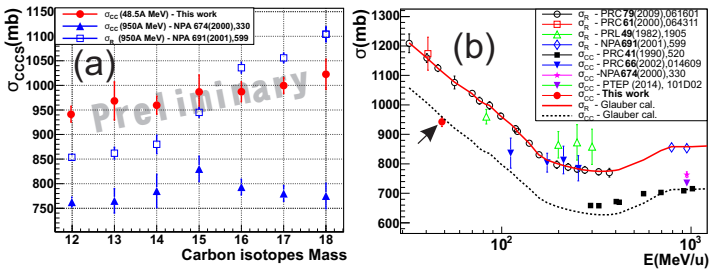

Figure 3: (a) The CCCS of carbon isotopes. (b) Reaction cross section and CCCS of ^{12}C.

as shown in eq. 2.

$$\sigma_{\rm CC} = \frac{1}{t} \ln \left[\frac{\gamma_{out}(1 - P_{in})}{\gamma_{in}(1 - P_{out})} \right] \tag{2}$$

where *in* and *out* indicate measurements with and without target respectively. This is the main difference in data analysis from the high energy experiment. The P_i $(i : in, out)$ was calculated by considering Rutherford scattering of the incident beam in the target. The difference in solid angle $(\Delta\Omega)$ covered by a particular layer (MUSIC electrode) but not by the next layer (MUSIC electrode or NaI(Tl)), was calculated. The number of beam with signal in one layer of MUSIC but without signal in next layer was considered as the number of particles scattered into the solid angle $\Delta\Omega$. The ratio $\Delta N/(\Delta\Omega N_{\rm inc})$ is proportional to the differential cross sections of scattered particles and was fitted with Rutherford distribution. The area below distribution curve from the maximum angle covered by NaI to 180 degree is the P_i (the shadowed in fig. 2(c)). We note that the assumed Rutherford distribution is consistent with the experiment data, as well as with a Monte Carlo simulation using the GEANT4 code (fig. 2(c)). The calculated P_{in} value varies from 0.003 to 0.004, resulting in 2 to 10% uncertainty, and the P_{out} value varies from 0.0005 to 0.0012, resulting in 5 to 15% uncertainty. These uncertainties result in systematic uncertainty of 6 - 10 mb for the $\sigma_{\rm CC}$ for difference isotopes. The determined CCCS's for $^{12-18}$C isotopes are shown in fig. 3(a). The error bar includes the above-mentioned systematic uncertainty, the statistical uncertainty as well as the uncertainty in the target thickness ($< 0.43\%$). For comparison, $\sigma_{\rm CC}$'s and $\sigma_{\rm R}$'s for the same isotopes at 950A MeV are also shown.

For $^{12-18}$C, our $\sigma_{\rm CC}$'s are almost constant in contrast with $\sigma_{\rm R}$'s. This trend is consistent with the AMD predictions [10]. Our results also qualitatively agree with the ones at 950A MeV for $^{12-15}$C; both results show different systematics for $^{16-18}$C.

It is important to note that we have applied the Glauber model adopting the finite-range optical limit approximation. To eliminate possible system-

atic error due to the energy dependence, we have fine-tuned the Glauber model so as to reproduce $\sigma_{\rm R}$ for ^{12}C on ^{12}C target at various energies as well as for $\sigma_{\rm CC}$ at 50A MeV. Fig. 3(b) shows $\sigma_{\rm R}$ and $\sigma_{\rm CC}$ for ^{12}C on ^{12}C target at energies up to 950A MeV. Except the points between $300A-500A$ MeV, $\sigma_{\rm CC}$'s at higher energies are also reproduced relatively well by our Glauber model calculations. It will interesting to compare our results with $\sigma_{\rm CC}$'s for $^{12-18}$C at 800A MeV [14].

4 Summary

We have measured the Charge-Changing Cross Sections (CCCS's) of $^{12-18}$C on a ^{12}C target at 50A MeV at the RCNP EN Course in Osaka University. We have shown, for the first time, the possibility to extend the Glauber model to the $\sigma_{\rm CC}$ measurements to determine the proton distribution radii of nuclei.

References

[1] L. -B Wang *et al.*, *Phys. Rev. Lett.*, **93** (2004) 142501.

[2] R. Sanchez *et al.*, *Phys. Rev. Lett.*, **96** (2006) 033002.

[3] P. Mueller, *Phys. Rev. Lett.*, **99** (2007) 252501.

[4] W. Nortershauser *et al.*, *Phys. Rev. Lett.*, **102** (2009) 062503.

[5] A. Ozawa *et al.*, *Nucl. Phys. A*, **691** (2001) 599.

[6] I. Tanihata *et al.*, *Prog. Part. Nucl. Phys.*, **68** (2013) 215.

[7] S. Terashima *et al.*, *Prog. Theor. Exp. Phys.* (2014) 101D02,.

[8] A. Estrade *et al.*, *Phys. Rev. Lett.*, **113** (2014) 132501.

[9] T. Yamaguchi *et al.*, *Phys. Rev. Lett.*, **107** (2011) 032502.

[10] Y. Kanada-En'yo, *Phys. Rev. C*, **91** (2015) 014315.

[11] T. Shimoda *et al.*, *Nucl. Instr. Methods Phys. Res. B*, **70** (1992) 320.

[12] H. Kumagai *et al.*, *Nucl. Instr. Methods Phys. Res. A*, **470** (2001) 562.

[13] K. Kimura *et al.*, *Nucl. Instr. Methods Phys. Res. A*, **538** (2005) 608.

[14] R. Kanungo *et al.*, *GSI-S395 experiment proposal* (2010).